Published in final edited form as:
*J Polym Sci A Polym Chem*. 2012 March 1; 50(5): 890–899. doi:10.1002/pola.25841.

# A series of poly[*N*-(2-hydroxypropyl)methacrylamide] copolymers with anthracene-derived fluorophores showing aggregation-induced emission properties for bioimaging

**Hongguang Lu**[1,2], **Fengyu Su**[1], **Qian Mei**[1], **Xianfeng Zhou**[1], **Yanqing Tian**[1,*], **Wenjing Tian**[2], **Roger H. Johnson**[1], and **Deirdre R. Meldrum**[1]

[1]Center for Biosignatures Discovery Automation, Biodesign Institute, Arizona State University, Tempe, AZ 85287, USA

[2]State Key Laboratory of Supramolecular Structure and Materials, College of Chemistry, Jilin University, Changchun 130012, PR China

## Abstract

A series of new poly[*N*-(2-hydroxypropyl)methacrylamide]-based amphiphilic copolymers were synthesized through a radical copolymerization of a monomeric/hydrophobic fluorophore possessing aggregation-induced emission (AIE) property with *N*-(2-hydroxypropyl)methacrylamide. Photophysical properties were investigated using UV-Vis absorbance and fluorescence spectrophotometry. Influences of the polymer structures with different molar ratios of the AIE fluorophores on their photophysical properties were studied. Results show that the AIE fluorophores aggregate in the cores of the micelles formed from the amphiphilic random copolymers and polymers with more hydrophobic AIE fluorophores facilitate stronger aggregations of the AIE segments to obtain higher quantum efficiencies. The polymers reported herein have good water solubility, enabling the application of hydrophobic AIE materials in biological conditions. The polymers were endocytosed by two experimental cell lines, human brain glioblastoma U87MG cells and human esophagus premalignant CP-A, with a distribution into the cytoplasm. The polymers are non-cytotoxic to the two cell lines at a polymer concentration of 1 mg/mL.

### Keywords

biopolymers; self-assembly; dyes; fluorescence; imaging

## 1. Introduction

Fluorescence based optical imaging plays a crucial role for biological investigation, for example, for the understanding of biological processes, metabolism and pharmacokinetics, as well as the diagnosis/detection of disease and cancer formation either *in vitro* or *in-vivo*. Many fluorescent probes are suitable for optical imaging. Typical fluorescent probes include but are not limited to fluorescein derivatives,[1] rhodamines,[1] cyanine derivatives,[1] quantum dots,[1] indocyanine greens (ICGs),[2,3] upconversion nanoparticles,[4–6] and two-photon absorbing materials.[7–14] In general, these fluorescent probes work well for bioimaging. However, most of these probes suffer a common problem. If the concentration is too high, many of the above mentioned fluorescent probes tend to form aggregates, causing aggregation-induced quenching (AIQ) to reduce fluorescence intensity.[15–18] This AIQ effect

*To whom all correspondence should be addressed. Phone: 480-965-9601. Fax: 480-727-6588. yanqing.tian@asu.edu.

impedes the performance for bioimaging. Recently, a new category of fluorophores with exactly the opposite characteristic to the AIQ, aggregation-induced emission (AIE), has been developed. AIE fluorophores have been shown to have high fluorescence quantum yields in the aggregated states.[19–25] Restricted intramolecular motion has been suggested as the possible mechanism of AIE phenomenon. The vibrational/torsional motions of the molecules affect drastically the radiative/nonradiative recombination processes of the excited state. In biological research fields, AIE fluorophores have been widely explored as sensors for DNA,[26, 27] heparin,[28] ATP,[29] pH,[30,31] $CO_2$,[32] and glucose.[33] Fewer studies were reported about the applications of the AIE fluorophores as bioimaging probes[34–39] than those about light emitting diodes and biosensors. This is mainly because that most of the AIE fluorophores are hydrophobic, limiting their applications in biological environments. Chemical modification of the AIE fluorophores with polar functional groups can improve their solubility/dispersion in aqueous media.[31,40,41] Nevertheless, most of these chemical modifications not only require complicated synthetic procedures, but also sometimes lower the fluorescence quantum efficiencies due to quenching of their excited states by water and nonradiative decay of the excited dyes in aqueous media.[42] A few advanced approaches have been used to alleviate these problems and enable the use of AIE fluorophores for bioimaging.[34–39] Nanoparticles such as organically modified silica nanoparticles[34–37] and amphiphilic block copolymers-based micelles[38] were utilized as nanocarriers to deliver hydrophobic AIE probes into cells. Besides the physical incorporation of hydrophobic AIE fluorophores into nanoparticles, AIE fluorophores were chemically conjugated to silica nanoparticles[36] and biocompatible hydrophilic glycol chitosan for bioimaging.[39] We have recently reported a class of 9,10-distyrylanthracene (DSA) derivatives with AIE properties.[25] The investigation indicates that the restricted intramolecular rotations between the 9,10-anthylene core and the vinylene segment are the cause for the AIE phenomenon. We also used anthracene derived materials as typical AIE fluorophores for pH and DNA sensing.[31] Herein, we report the development and bioapplication of a new series of AIE-fluorophore-containing random copolymers, polymerized from an AIE fluorophore with a styrene moiety as a monomer (AIEM, Scheme 1), *N*-(2-hydroxypropyl)methacrylamide (HPMA), and 2-aminoethyl methacrylate (AEMA). Poly[*N*-(2-hydroxypropyl)methacrylamide] (PHPMA) is a biocompatible polymer with little or non-cytotoxicity, and has been widely applied in biological research fields of drug delivery, *in-vivo* imaging, and photodynamic therapy.[43–45] The use of poly(2-aminoethyl methacrylate ) (PAEMA) is to enhance the cellular uptake of the polymers by using cationic amino groups.[46–48] Thus, in light of the development of AIE fluorophores for bioimaging, we will for the first time report the preparation of biocompatible AIE-fluorophore-containing random copolymers for bioimaging. Through the tuning of polymeric structures and the molar ratios of AIE fluorophores in the copolymers, polymer structure-dependent optical properties were investigated. Bioimaging of the polymers for two cell lines (human brain glioblastoma U87MG cells and human esophagus premalignant CP-A) was investigated. Considering the simple approach of the preparation of random copolymers with AIE fluorophores and the abundant biocompatible polymer structures, it is expected that the polymer approach will enable the wide application of hydrophobic AIE fluorophores for bioimaging.

## 2. Experimental

### 2.1 Materials and reagents

All chemicals and solvents were of analytical grade and were used without further purification. Tetrahydrofuran (THF), *N*,*N*′-dimethylformamide (DMF), dimethyl sulfoxide (DMSO), azobisisobutyronitrile (AIBN), anthracene, potassium tert-butoxide (KOtBu), n-hexyl bromide, potassium carbonate, 6-chloro-1-hexanol, potassium iodide, 4-vinylbenzyl chloride, sodium hydride (NaH), 2-aminoethyl methacrylate hydrochloride (AEMA), and 4-

(2-hydroxyethyl)-1-piperazineethanesulfonic acid (HEPES) were commercially available from Sigma-Aldrich (St. Louis, MO) and were used without further purification. Monomer HPMA was prepared according to the known procedure.[43–45] Tetraethyl anthracene-9,10-bis(methylene)phosphonate (compound **1**) and 4-tetrahydro-pyran-2-yloxy-benzaldehyde (compound **2**) were synthesized according to known procedures.[49, 50]

Eagle's minimum essential medium (EMEM) and Keratinocyte medium were purchased from Invitrogen (Carlsbad, CA). EMEM was used for U87 cell culture. Keratinocyte medium was used for CP-A cell culture. 3-(4,5-Dimethyl thiazol-2-yl)-2,5-diphenyltetrazolium bromide (MTT) assay was purchased from Promega (Madison, WI).

### 2.2 Instruments

A Varian liquid-state NMR operated at 400 MHz for $^{1}$H NMR and 100 MHz for $^{13}$C NMR was used for NMR spectra measurements. High resolution mass spectrometry (HRMS) was performed by the ASU Mass Spectrometry Laboratory. A Shimadzu UV-3600 UV-VIS-NIR spectrophotometer (Shimadzu Scientific Instruments, Columbia, MD) was used for absorbance measurements. A Shimadzu RF-5301 spectrofluorophotometer was used for fluorescence measurements. Waters 1515 GPC coupled with a RI detector, in reference to a series of poly(2-vinylpyridine) standards in 5% acetic acid aqueous solution as the eluent, was used for polymer molecular weight determination. Dynamic light scattering (DLS) measurements were performed using a 173° back scattering Malvern Nano-ZS instrument. The solution was filtered through a 0.45 μm Millipore Millex-HN filter to remove dust before DLS measurements. Atomic force microscopy (AFM, NanoScope III, Digital Instrument) equipped with an integrated silicon tip/cantilever with a resonance frequency of ~240 kHz in height image model was utilized for the observation of morphologies. Polymer solutions (4 μL) were dropped on a mica sample stage and dried at room temperature for the morphological observation. The AFM topographies showed no evidence of tip-induced modification during successive scans.

### 2.3 Synthesis

Synthesis of 9,10-bis(4-(tetrahydro-2H-pyran-2-yloxy)styryl)anthracene **(3)**. 2.40 g of compound **1** (5.0 mmol) and 1.68 g of potassium tert-butoxide (15.0 mmol) were dissolved in 100 mL of anhydrous THF. A solution of 2.47 g of compound **2** (12.0 mmol) in 20 mL of anhydrous THF was added dropwisely over a 20 min at 0 °C. The resultant mixture was allowed to warm to room temperature and then stirred overnight. After solvent evaporation, the residue was redissolved into 5 mL of $CH_2Cl_2$ and reprecipitated into 200 mL of methanol to afford a yellow solid (2.18 g, 75% yield). $^{1}$H NMR ($CDCl_3$, 400 MHz), δ (TMS, ppm): 8.37–8.39 (m, 4H), 7.78 (d, J =16.5Hz, 2H), 7.60 (d, J = 8.5 Hz, 4H), 7.43–7.46 (m, 4H), 7.13 (d, J = 8.5Hz, 4H), 6.86 (d, J = 16.5Hz, 2H), 5.50 (t, 2H), 3.91–3.97 (m, 2H), 3.61–3.66 (m, 2H), 1.89–2.05 (m, 4H), 1.55–1.71 (m, 8H); $^{13}$C NMR (DMSO-$d_6$, 100 MHz), δ (TMS, ppm): 156.97, 136.86, 132.74, 130.98, 129.58, 127.66, 126.49, 125.06, 123.15, 116.78, 96.30, 61.99, 30.30, 25.20, 18.71; HRMS (APCI+): $C_{40}H_{39}O_4$ (M+H), calcd. 583.2848; found 583.2839.

Synthesis of 9,10-bis(4-hydroxystyryl)anthracene **(4)**. 1.75 g of compound **3** (3.0 mmol) was dissolved into 100 mL of THF and 5 mL of methanol, and then 10 mL of 2 N HCl aqueous solution was added into the solution. The reaction mixture was stirred at room temperature for 12 h. After the solvent was removed under reduced pressure, the residue was washed with methanol. The solid was redissolved into 5 mL of $CH_2Cl_2$ and reprecipitated into 200 mL of methanol to give a yellow solid (1.10 g, 88% yield). $^{1}$H NMR (DMSO-$d_6$, 400 MHz), δ (TMS, ppm): 9.67 (s, 2H), 8.32–8.34 (m, 4H), 7.83 (d, J =16.5Hz, 2H), 7.60 (d, J = 8.5Hz, 4H), 7.48–7.51 (m, 4H), 6.82 (d, J = 8.5Hz, 4H), 6.77 (d, J = 16.5Hz, 2H); $^{13}$C NMR

(DMSO-$d_6$, 100 MHz), δ (TMS, ppm): 157.61, 137.03, 132.36, 128.98, 128.09, 128.06, 126.22, 125.31, 121.11, 115.55; HRMS (APCI+): $C_{30}H_{23}O_2$ (M+H), calcd. 415.1698; found 415.1699.

Synthesis of 4-((E)-2-(10-(4-(hexyloxy)styryl)anthracen-9-yl)vinyl)phenol **(5)**. Into a 25 mL round-bottomed flask were added 0.42 g of compound **4** (1.0 mmol) and 0.21 g of $K_2CO_3$ (1.5 mmol) in 10 mL of anhydrous DMF. A solution of 0.15 g of 1-bromohexane (0.9 mmol) in 2 mL of DMF was added to the mixture under stirring. The mixture was stirred for 12 h at 60 °C. After being cooled to room temperature, the reaction mixture was poured into water and extracted with $CH_2Cl_2$ (3 × 40 mL). The combined organic extracts were washed with brine, dried over $MgSO_4$, and concentrated to dryness under vacuum. The crude product was purified by silica gel chromatography ($CH_2Cl_2$) to give a yellow solid (0.23 g, 45% yield). $^1$H NMR ($CDCl_3$, 400 MHz), δ (TMS, ppm): 8.37–8.40 (m, 4H), 7.76 (d, J =16.5Hz, 2H), 7.56–7.61 (m, 4H), 7.43–7.46 (m, 4H), 6.97 (d, J = 8.5Hz, 2H), 6.91 (d, J = 8.5Hz, 2H), 6.83–6.88 (m, 2H), 4.79 (s, 1H), 4.02 (t, 2H), 1.78–1.85 (m, 2H), 1.34–1.51 (m, 6H), 0.917 (t, 3H); $^{13}$C NMR ($CDCl_3$, 100 MHz), δ (TMS, ppm): 159.15, 155.44, 136.90, 136.69, 132.86, 132.62, 130.45, 129.96, 129.60, 127.99, 127.75, 126.53, 126.46, 125.09, 125.05, 123.01, 122.69, 115.67, 114.81, 68.18, 31.60, 29.23, 25.73, 22.62, 14.06; HRMS (APCI+): $C_{36}H_{35}O_2$ (M+H), calcd. 499.2637; found 499.2638.

Synthesis of 6-[4-(2-{10-[2-(4-hexyloxy-phenyl)-vinyl]-anthracen-9-yl}-vinyl)-phenoxy]-hexanol **(6)**. Into a 25 mL round-bottomed flask were added 1.20 g of compound **5** (2.4 mmol) and 0.50 g of $K_2CO_3$ (3.6 mmol) in 10 mL of anhydrous DMF. A solution of 0.52 g of 6-chloro-1-hexanol (2.9 mmol) in 2 mL of DMF was added to the mixture under stirring. The mixture was stirred for 12 h at 60 °C. After being cooled to room temperature, the reaction mixture was poured into water and extracted with $CH_2Cl_2$ (3 × 50 mL). The combined organic extracts were washed with brine, dried over $MgSO_4$, and concentrated to dryness under vacuum. The crude product was purified by silica gel chromatography ($CH_2Cl_2$) to give a yellow solid (0.75 g, 52% yield). $^1$H NMR ($CDCl_3$, 400 MHz), δ (TMS, ppm): 8.38–8.40 (m, 4H), 7.75–7.81 (m, 2H), 7.59–7.63 (m, 4H), 7.44–7.46 (m, 4H), 6.97–7.00 (m, 4H), 6.84–6.90 (m, 2H), 4.01–4.04 (m, 4H), 3.66–3.70 (m, 2H), 1.82–1.86 (m, 4H), 1.36–1.49 (m, 12H), 0.92 (t, 3H); $^{13}$C NMR ($CDCl_3$, 100 MHz), δ (TMS, ppm): 159.15, 159.07, 136.88, 136.84, 132.78, 132.75, 130.03, 129.96, 129.60, 127.74, 126.50, 125.04, 122.77, 122.70, 114.79, 68.10, 67.97, 62.92, 32.69, 31.60, 29.23, 25.90, 25.72, 25.55, 22.62, 14.05; HRMS (APCI+): $C_{42}H_{47}O_3$ (M+H), calcd. 599.3525; found 599.3528.

Synthesis of 9-(4-(hexyloxy)styryl)-10-(4-(6-(4-vinylbenzyloxy)hexyloxy)styryl)anthracene **(AIEM)**. 1.20 g of compound **6** (2.0 mmol) was dissolved in 10 mL of anhydrous DMF. 0.46 g of 4-vinylbenzyl chloride (3.0 mmol) and 0.80 g of 60% NaH in mineral oil (20.0 mmol) were added into the reaction mixture under $N_2$ atmosphere. The mixture was stirred for 12 h at 60 °C. After being cooled to room temperature, the reaction mixture was poured into water and extracted with $CH_2Cl_2$ (3 × 50 mL). The combined organic extracts were washed with brine, dried over $MgSO_4$, and concentrated to dryness under vacuum. The crude product was purified by silica gel chromatography (Hexane: $CH_2Cl_2$ = 5:1) to give a yellow solid (1.16 g, 81% yield). $^1$H NMR ($CDCl_3$, 400 MHz), δ (TMS, ppm): 8.38–8.40 (m, 4H), 7.76 (d, J =16.5Hz, 2H), 7.59 (d, J = 8.5 Hz, 4H), 7.44–7.46 (m, 4H), 7.38 (d, J = 8.5Hz, 2H), 7.29 (d, J = 8.5Hz, 2H), 6.95–6.98 (m, 4H), 6.85 (d, J = 16.5Hz, 2H), 6.67–6.74 (m, 1H), 5.73 (d, 1H), 5.21 (d, 1H), 4.45 (s, 2H), 4.02 (t, 4H), 3.48 (t, 2H), 1.82 (m, 4H), 1.66 (m, 2H) 1.48 (m, 6H), 1.35 (m, 4H), 0.92 (t, 3H); $^{13}$C NMR ($CDCl_3$, 100 MHz), δ (TMS, ppm): 159.17, 159.12, 136.89, 136.58, 132.79, 130.01, 129.98, 129.62, 127.83, 127.76, 126.53, 126.21, 125.06, 122.75, 122.73, 114.82, 113.70, 72.62, 70.27, 68.18, 68.03, 31.62, 29.72, 29.25, 29.23, 26.03, 25.93, 25.75, 22.64, 14.07; HRMS (APCI+): $C_{51}H_{55}O_3$ (M+H), calcd. 715.4151; found 715.4144.

Synthesis of poly(*N*-(2-hydroxypropyl) methacrylamide)-*co*-poly(2-aminoethyl methacrylate)-*co*-poly[4-[6-[4-(2-{10-[2-(4-hexyloxy-phenyl)-vinyl]-anthracen-9-yl}-vinyl)-phenoxy]-hexyloxymethyl] styrene} (**P1**) with molar ratios of x:y:z of 100: 3.5: 1. 500 mg of HPMA, 20 mg of AEMA, 25 mg of AIEM, and 10 mg AIBN were dissolved in 5 mL of DMF. The solution was degassed three times through a standard freeze-thaw process. The monomers were polymerized at 65 °C for 20 hours under nitrogen. Polymer was precipitated into 200 mL of ether from the DMF solution. After filtration, the polymer was redissolved in 10 mL DMF and reprecipitated into 100 mL of ether. Yield: 410 mg (75%). $M_n$ = 11200, $M_w$ = 15800, $M_w/M_n$ = 1.41. $^1$H NMR (DMSO-$d_6$, 400 MHz), δ (TMS, ppm): 7.01–8.39 (broad, aromatic protons), 4.68 (broad, -$CH_2$OCO), 4.00 (broad, -$CH_2$O-), 3.64 (broad, -$CH_2$NH-), 2.85 (broad, -$CH_2$CO-), 1.41–2.01 (broad, backbone protons, -$(CH_2)_5$-), 1.08 (broad, -$CH_3$).

Synthesis of poly(*N*-(2-hydroxypropyl) methacrylamide)-*co*-poly(2-aminoethyl methacrylate)-*co*-poly[4-[6-[4-(2-{10-[2-(4-hexyloxy-phenyl)-vinyl]-anthracen-9-yl}-vinyl)-phenoxy]-hexyloxymethyl] styrene} (**P2)** with molar ratios of x:y:z of 100: 3.5: 2. Similar condition as **P1**, except the weight of AIEM used for this polymerization was 50 mg. Yield: 80%. $M_n$ = 11600, $M_w$ = 15200, $M_w/M_n$ = 1.31. $^1$H NMR (DMSO-$d_6$, 400 MHz), δ (TMS, ppm): 7.00–8.39 (broad, aromatic protons), 4.67 (broad, -$CH_2$OCO), 4.32 (broad, -$CH_2$O-Ph), 4.00 (broad, -$CH_2$O-), 3.64 (broad, -$CH_2$NH-), 2.85 (broad, -$CH_2$CO-), 1.41–2.01 (broad, backbone potons, -$(CH_2)_5$-), 0.98 (broad, -$CH_3$).

Synthesis of poly(*N*-(2-hydroxypropyl) methacrylamide)-*co*-poly(2-aminoethyl methacrylate)-*co*-poly[4-[6-[4-(2-{10-[2-(4-hexyloxy-phenyl)-vinyl]-anthracen-9-yl}-vinyl)-phenoxy]-hexyloxymethyl] styrene} (**P3**) with molar ratios of x:y:z of 100: 3.5: 4. Similar condition as **P1**, except the weight of AIEM used for this polymerization was 100 mg. Yield: 66%. $M_n$ = 11800, $M_w$ = 15700, $M_w/M_n$ = 1.33. $^1$H NMR (DMSO-$d_6$, 400 MHz), δ (TMS, ppm): 6.97–8.33 (broad, aromatic protons), 4.67 (broad, -$CH_2$OCO), 4.32 (broad, -$CH_2$O-Ph), 4.00 (broad, -$CH_2$O-), 3.64 (broad, -$CH_2$NH-), 2.85 (broad, -$CH_2$CO-), 1.21–1.87 (broad, backbone protons, -$(CH_2)_5$-), 1.01 (broad, -$CH_3$).

Synthesis of poly(*N*-(2-hydroxypropyl) methacrylamide)-*co*-poly(2-aminoethyl methacrylate)-*co*-poly[4-[6-[4-(2-{10-[2-(4-hexyloxy-phenyl)-vinyl]-anthracen-9-yl}-vinyl)-phenoxy]-hexyloxymethyl] styrene} (**P4**) with molar ratios of x:y:z of 100: 3.5: 8. Similar condition as **P1**, except the weight of AIEM used for this polymerization was 200 mg. Yield: 70%. $M_n$ = 30300, $M_w$ = 34800, $M_w/M_n$ = 1.16. $^1$H NMR (DMSO-$d_6$, 400 MHz), δ (TMS, ppm): 6.84–8.39 (broad, aromatic protons), 4.67 (broad, -$CH_2$OCO), 4.34 (broad, -$CH_2$O-Ph), 3.98 (broad, -$CH_2$O-), 3.64 (broad, -$CH_2$NH-), 2.85 (broad, -$CH_2$CO-), 1.11–1.88 (broad, backbone Hs, -$(CH_2)_5$-), 0.98 (broad, -$CH_3$).

Synthesis of poly(*N*-(2-hydroxypropyl) methacrylamide)-*co*-poly(2-aminoethyl methacrylate)-*co*-poly[4-[6-[4-(2-{10-[2-(4-hexyloxy-phenyl)-vinyl]-anthracen-9-yl}-vinyl)-phenoxy]-hexyloxymethyl] styrene} (**P5**) with molar ratios of x:y:z of 100: 3.5: 16. Similar condition as **P1**, except the weight of AIEM used for this polymerization was 400 mg. Yield: 83%. $M_n$ = 28500, $M_w$ = 33900, $M_w/M_n$ = 1.20. $^1$H NMR (DMSO-$d_6$, 400 MHz), δ (TMS, ppm): 6.68–8.30 (broad, aromatic protons), 4.67 (broad, -$CH_2$OCO), 4.32 (broad, -$CH_2$O-Ph), 4.00 (broad, -$CH_2$O-), 3.64 (broad, -$CH_2$NH-), 2.86 (broad, -$CH_2$CO-), 1.21–1.89 (broad, backbone protons, -$(CH_2)_5$-), 0.98 (broad, -$CH_3$).

### 2.4 Quantum efficiency measurements

Fluorescence quantum yields for the AIE fluorophores were obtained by comparing the integrated fluorescence spectra of the polymers in solutions to the fluorescence spectrum of

quinine sulfate in 1.0 N $H_2SO_4$ ($\Phi$ = 0.55, excitation wavelength of 365 nm)[51] with a correction of refractive index differences using equation 1.[52]

$$\eta_s = \eta_r \left(\frac{A_r}{A_s}\right)\left(\frac{I_s}{I_r}\right)\left(\frac{{n_s}^2}{{n_r}^2}\right) \quad (1)$$

where ($\eta_r$) and ($\eta_s$) are the fluorescence quantum yield of standards and the samples, respectively. $A_r$ and $A_s$ are the absorbance of the standards and the measured samples at the excitation wavelength, respectively. $I_r$ and $I_s$ are the integrated emission intensities of standards and the samples. $n_r$ and $n_s$ are the refractive indices of the corresponding solvents of the solutions, respectively (the refractive indexes of $H_2O$ and DMSO are 1.333 and 1.479, respectively). The final value of quantum yield was obtained from the average of four measurements with different absorbance in the range between 0.03 and 0.09. The standard deviation is less than 10%.

### 2.5 Culture of U87MG and CP-A cells for bioimaging

U87MG cells (American Type Culture Collection, ATCC, Manassas, VA) were cultured in EMEM supplemented with 10% fetal bovine serum, 5% penicillin, 2 mM L-glutamine (Sigma-Aldrich), and incubated at 37 °C in a 5% $CO_2$ atmosphere. CP-A cells (kindly provided by Dr. Brian J. Reid at Fred Hutchison Cancer Research Center, Seattle, WA) were cultured in Keratinocyte-serum free medium (Invitrogen, Carlsbad, CA) supplemented with Bovine Pituitary Extract (BPE) and human recombinant Epidermal Growth Factor (rEGF, Invitrogen) at 37 °C in a 5% $CO_2$ atmosphere. CP-A (also identified as KR-42421 or QhTERT) was derived from an endoscopic biopsy specimen obtained from a region of non-dysplastic metaplasia and transduced with the retroviral expression vector, pLXSN-hTERT, to create an immortalized cell line. Cells were seeded onto 96-well plates at 10,000 cells per well, and incubated for 1 day. Polymer **P4** dissolved in 10 mM HEPES buffers were added to the medium to make the AIE fluorophore concentration of 5 μM, corresponding to the polymer concentration of 0.013 mg/mL. After incubation at 37 °C for 24 hours, cells were washed using fresh medium and then used for bioimaging. Under Nikon Eclipse TE2000E confocal fluorescence microscope (Melville, NY), the polymers were excited at 402 nm and their green emission was collected using a 515/30 nm filter set.

### 2.6 MTT assay

The assay was performed by an in vitro MTT-based toxicology assay kit (Promega). U87MG cells were cultured in EMEM supplemented with 10% fetal bovine serum, 5% penicillin, and 2 mM L-glutamine (Sigma-Aldrich) at 37 °C in a 5% $CO_2$ atmosphere. CP-A cells were cultured in Keratinocyte-serum free medium at 37 °C in a 5% $CO_2$ atmosphere. U87MG and CP-A cells were seeded onto 96-well plates at 10,000 cells per well, and incubated for 1 day. The polymers in 10 mM HEPES buffers were added into the cell culture media to a final polymer concentration of 0.1 to 1.0 mg/mL and the cells with the polymers were incubated in the 96 well plates. Twenty four hours later, the medium in the wells were removed and the cells were washed with PBS buffer and then incubated in fresh medium (100 μL) and 10 μL of MTT solution (5 mg/mL) in 5% $CO_2$ at 37 °C for another 3 h. One hundred microlitters of stabilizer (Promega) was added to each well to dissolve the internalized purple formazan crystals by gentle pipetting up and down. The absorbance was measured at a wavelength of 570 nm using a SpectraMax 190 from Molecular Devices (Downingtown, PA). Each experiment was conducted twice in triplicate. The result was expressed as a percentage of the absorbance of the blank control.

### 2.7 Flow cytometric analysis

To demonstrate the time and temperature dependent cellular uptake of the polymers, fluorescence measurements were carried out by using a FACS caliber cytometer (Becton Dickinson Immunocytometry Systems, San Jose, CA). 125 °L of **P4** with AIE fluorophore concentration of 200 °M (polymer concentration was of 0.52 mg/mL) in HEPES buffer was added to about 1 million cells in 5 mL medium in the individual flow tubes. The mixture was incubated at 37 °C or 4 °C in a cell incubator for various time periods. After incubation, the cells were centrifuged, washed twice with fresh medium, and then suspended in fresh medium again. Fluorescence was determined by counting 10,000 events.

## 3. Results and discussion

### 3.1. Synthesis of AIE monomer and polymers

The AIE fluorophore was constructed from an anthracene derivative (compound **1**, Scheme 1). Through the condensation of **1** and **2**, compound **3** was obtained. Compound **4** was synthesized through the deprotection of the tetrahydropranyl units on **3** under mild acidic condition in methanol and THF. **4** was then reacted with 1-bromohexane to get a mono-hexyloxy-substituted **4**, i.e. compound **5**. Compound **6** was obtained by a reaction of **5** with 6-chloro-1-hexanol. Through a reaction of **6** with 4-vinylbenzyl chloride, the monomeric AIE fluorophore (AIEM) was obtained. This monomer was used to copolymerize with HPMA and AEMA under the normal radical polymerization conditions at 65 °C for 20 hours using AIBN as a thermal initiator to form a series of copolymers of **P1** to **P5**. The molar ratios of HPMA to AEMA were kept constant of 100:3.5 (Scheme 1), while the AIEM molar ratio to the sum of HPMA and AEMA was increased from 1.0:103.5 for **P1** to 16.0:103.5 for **P5**. Thus, the influence of AIEM molar fractions on the photophysical properties could be investigated. The polymers have very good solubility in DMSO and DMF with a concentration of at least 50 mg/mL. After dispersing the DMSO solution into water or HEPES buffer and removing the DMSO using dialysis, the polymers can be dissolved in aqueous solutions with a concentration of at least 10 mg/mL.

### 3.2. Photophysical properties and possible nanostructures

Figure 1A shows the typical absorbance and emission spectra of **P3** in DMSO and in DMSO/$H_2O$ (2:98 by volume). The polymer in DMSO has almost no emission with quantum efficiency of 0.08%. At the same polymer concentration, with the increase of water fraction in DMSO, the absorbance decreases and the fluorescence intensity increases (Figure 1B). These phenomena were observed in other AIE materials,[26, 27, 31] suggesting the typical AIE characteristics. The quantum efficiency of **P3** in DMSO/$H_2O$ (2:98 by volume) increased to 7.9%, which is 98 fold greater than that in pure DMSO. Figure 1C shows the typical quantum efficiencies of the polymers **P1**–**P5** at the DMSO/$H_2O$ mixtures, indicating materials dependent photophysical properties. DMSO is a strong solvent for all the polymer segments, PHPMA, PAEMA, and PAIE. The AIE fluorophores can rotate freely in the strong solvent of DMSO to lose their energies to result in their extremely weak emission intensities. With the addition of water into the polymer solutions in DMSO, the hydrophobic AIE fluorophores started to reassemble with the hydrophilic PHEMA and PAEMA polymer chains, possibly through the formation of micellar nanostructures (Figure 2). The hydrophobic PAIE segments aggregate together as the hydrophobic cores, limiting or restricting the intramolecular rotations of the AIE fluorophores to increase the fluorescence quantum efficiencies. With more water fractions, the aggregations become stronger. From Figure 1C, it can be seen that, for the polymers with more hydrophobic PAIE segments, the aggregations of the PAIE segments start earlier with lower water fractions. At the same DMSO/$H_2O$ fraction, the polymers with higher AIE fractions exhibit higher quantum efficiencies of the PAIE fluorophores. When the AIE fluorophore's fraction reaches a certain

level, for example over the molar fraction of **P4**, the quantum efficiency change is not significant with the further increase of AIE fractions.

It should be noted here, the organic small molecule-based anthracene AIE dyes formed J-aggregations (31), which was observed by the red-shift of absorption maximum at the aggregated states while without obvious emission maximum changes. In the AIE-containing polymers, the J-aggregations were not obvious. Most likely, the stoichiometry of the polymer main and side chains interfered the fluorophores' interactions and aggregations.

In order to determine whether these polymers can form nanostructures, two typical polymer solutions of **P1** and **P4** were measured using dynamic light scattering (DLS). The absence of reliable scattering data of these polymers in DMSO indicated their unimer structures. Small particles with diameters of 11.0 ± 3 nm for **P1** and 10.4 ± 4 nm for **P4** in DMSO/$H_2O$ (2:98 by volume) were observed (Figure 2A), suggesting the polymers' aggregated nanostructures (Figure 2B). Considering the AIE fluorophore has a longer molecular length than the HPMA (the fully extended lengths of AIE monomer and HPMA are 3.6 nm and 0.6 nm respectively, calculated using ChemDraw 3D software), we proposed the micelle structures using the “flower micelle model” reported by Tominage et al.[53] Such micelles can be formed through an aggregation of the AIE probes as the micelle cores and the entangled PHPMA/PAEMA chains as the hydrophilic loop-like shells (Figure 2B). According to this model, if the polymers are packed tightly, the diameters are about 8.4 nm, which is quite close to the diameters (10 to 11 nm) measured using DLS. The 8.4 nm was calculated by using a double of a radius of 4.2 nm (3.6 nm + 0.6 nm) of the fully extended AIE monomer and HPMA. Because the hydrophilic shells formed from PHEMA and PAEMA chains may contain significant amount of water to extend the thickness of shells, the hydrophilic chains may entangle in the shell, and also the polymers are usually not packed tightly in solutions, the calculated sizes may usually be smaller than those measured by DLS. The “flower micelle model” can also explain that the diameters of the micelles are neither significantly affected by the molar fractions ratios of the AIE fluorophores in the polymers, nor by the polymeric molecular weights. Further confirmation of the micelles was visualized under AFM using **P4** as an example at its dry state. Small spherical micelles (Figure 2A, inserted figure) with an average diameter of 35 nm ± 15 were observed. The size is larger than the average diameter measured using DLS, which is probably due to the flattening of the micelles on the mica surface during the drying process.

Some random copolymers with both the hydrophilic and hydrophobic units were reported to form micelles having average diameters ranging from a few nanometers to hundreds nanometers with the hydrophobic segments as the micellar cores and hydrophobic chains as the shells.[48, 53–56] Critical micellar concentration (CMC) is an important factor for determination of micelles formation. For the fluorescent polymers, CMCs can be determined by the measurement of the concentration dependent fluorescence in aqueous solutions.[48] For the AIE polymers, before the micelle formation, the fluorophores have no aggregation and very weak fluorescence will be observed. Once the micelle is formed, the hydrophobic AIE fluorophores will aggregate, resulting in the observation of fluorescence. Meanwhile the fluorescence intensities after CMC will increase with the increase of concentrations. Fluorescence intensities at 539 nm were plotted against the polymer concentrations in aqueous solutions (Figure 3). It was found the CMCs of **P1** and **P4** are 0.031 mg/mL and 0.011 mg/mL, respectively. **P4** has more hydrophobic AIE segments than **P1**, exhibiting a lower CMC value than **P1**. It has been known that the CMC values depend on polymer structures, molecular weights, and the fractions of hydrophobic segments to hydrophilic segments. Some random copolymers were reported to have high CMCs of 2.0 mg/mL.[55] Some other random copolymers were reported to have much lower CMCs of around $5.3 \times 10^{-4}$ mg/mL.[56] Our polymers' CMCs are within the reported ranges.

### 3.3 Bioimaging

Figure 4 shows the confocal fluorescence microscopy images of one typical polymer (**P4**) for two cell lines (U87MG and CP-A) after 24 hour internalization with cells at 37°C. Green emission was observed, which is randomly distributed in the cytoplasma area of the cells, showing that the polymer in the form of micelles was successfully taken up by the cells and the AIE fluorophores were in the aggregated states. Similar results were observed for other polymers.

### 3.4 Time and temperature dependent flow cytometry

In order to understand the possible cellular uptake mechanism, flow cytometry was used to measure the fluorescence of the cells after internalization with the polymers. **P4** was used as a typical polymer. Figure 5A and 5B gave the time dependent fluorescence of the polymer internalized with cells at 37°C. Results showed that the fluorescence, which is due to the cellular uptake of the polymer, becomes stronger under longer cellular internalization time. This result suggests the cellular uptake of the polymer is time dependent. Figure 5C gives the time dependent fluorescence of the polymer internalized with cells at 4°C by CP-A cells. Comparing Figure 5B with Figure 5C, it can be found under the same cellular internalization time more polymers were taken up by cells at a higher temperature (37 °C) than at a lower temperature (4 °C). These results showed that the cellular internalization of the polymer is energy dependent. This characteristic suggests the endocytosis mechanisms of the cellular internalization of the polymer, which is time and energy dependent.[57–63] It should be noted here that the average diameters of the micelles and CMCs of the polymers were not significantly affected by temperatures at 4, 23, and 37 °C.

### 3.5 Cytotoxicity evaluation using MTT assay

MTT assay is based on the intracellular reduction of a tetrazolium (MTT) dye to a formazan product measured spectrophotometrically and is used for high-throughput screening.[64, 65] Figure 6 shows the typical cell viability of two polymers of **P1** and **P4** for U87MG and CP-A cells after cellular internalization for 24 hours at 37 °C. Higher than 95% of cell viability was observed after cellular internalization with a polymer concentration of up to 1.0 mg/mL for 24 hours. These studies showed the biocompatibility of the polymers.

## 4. Conclusion

A new series of PHPMA based random copolymers with hydrophobic AIE fluorophores were prepared. The increase of the molar fractions of the hydrophobic AIE fluorophores results in the higher quantum efficiencies of the AIE-containing copolymers. These polymers had almost no emissions in their strong solvents of DMSO, but showed fluorescence in the DMSO/water mixtures. These polymers were confirmed to form small micelles with average diameters of around 10 nm in their aqueous solutions. The polymers were cell permeable and were located in the cytoplasma area of U87MG and CP-A cells. The polymers did not show obvious cytotoxicity to the two experimental cell lines after cellular internalization for 24 hours with a polymer concentration up to 1 mg/mL. The cellular uptake of the polymer is time and energy dependent, indicating the endocytosis cellular internalization mechanism. Although the AIE fluorophore is water insoluble, its chemical conjugation with biocompatible polymers such as the PHPMA enables its application in biological condition for bioimaging and endows the non-cytotoxicity to cells.

## Acknowledgments

This work was supported by NIH National Human Genome Research Institute, Centers of Excellence in Genomic Science, Grant Number 5 P50 HG002360, Dr. Deirdre Meldrum, PI, Director. Dr. Brian J. Reid and Dr. Tom

Paulson at Fred Hutchison Cancer Research Center (Seattle, WA) were acknowledged for kindly providing us the CP-A cell line. Hongguang Lu thanks China Scholarship Council scholarship program for overseas graduate students.

## References

1. Johnson, I.; Spence, MTZ. The Molecular Probes Handbook-A Guide to Fluorescent Probes and Labeling Technologie. 11th ed.. Carlsbad, CA: 2010.
2. Bouteiller C, Clave G, Bernardin A, Chipon B, Massonneau M, Renard P-Y, Romieu A. Bioconjugate Chem. 2007; 18:1303–1317.
3. Buckle T, Chin PTK, Leeuwen FWB. Nanotechnology. 2010; 21:482001–482009. [PubMed: 21063057]
4. Chatterjee DK, Rufaihah AJ, Zhang Y. Biomaterials. 2008; 29:937–943. [PubMed: 18061257]
5. Vinegoni C, Razansky D, Ntziachristos V, Weissleder R. Opt Lett. 2009; 34:2566–2568. [PubMed: 19724491]
6. Xiong LQ, Chen ZG, Yu MX, Li FY, Liu C, Huang CH. Biomaterials. 2009; 30:5592–5600. [PubMed: 19564039]
7. Albota M, Beljonne D, Bredas JL, Ehrlich JE, Fu JY, Heikal AA, Hess SE, Kogej T, Levin MD, Marder SR, McCord-Maughon D, Perry JW, Röckel H, Rumi M, Subramaniam G, Webb WW, Wu XL, Xu C. Science. 1998; 281:1653–1656. [PubMed: 9733507]
8. So PTC, Dong CY, Masters BR, Berland KM. Annu Rev Biomed Eng. 2000; 2:399–429. [PubMed: 11701518]
9. Woo HY, Korystov D, Mikhailovsky A, Nguyen T-Q, Bazan GC. J Am Chem Soc. 2005; 127:13794–13795. [PubMed: 16201792]
10. Law WC, Yong KT, Roy I, Xu G, Ding H, Bergey EJ, Zeng H, Prasad PN. J Phys Chem C. 2008; 112:7972–7977.
11. Zhang X, Li W, Li X, Liu T, Fan Z, Yang W. J Polym Sci Part A: Polym Chem. 2010; 48:5704–5711.
12. Kim HM, Cho BR. Chem Asian J. 2011; 6:58–69. [PubMed: 20963746]
13. Tian YQ, Wu W-C, Chen C-Y, Jang S-H, Zhang M, Strovas T, Anderson J, Cookson B, Li Y, Meldrum D, Chen WC, Jen AK-Y. J Biomed Mater Research A. 2010; 93A:1068–1079. [PubMed: 19753625]
14. Tian YQ, Chen C-Y, Cheng Y-J, Young AC, Tucker NM, Jen AK-Y. Adv Funct Mater. 2007; 17:1691–1697.
15. Birks, JB. Photophysics of Aromatic Molecules. Wiley; London, UK: 1970.
16. Kraft A, Grimsdale AC, Holmes AB. Angew Chem Int Ed. 1998; 37:402–428.
17. Deans R, Kim J, Machacek MR, Swager TM. J Am Chem Soc. 2000; 122:8565–8566.
18. Suzuki Y, Yokoyama K. J Am Chem Soc. 2005; 127:17799–17802. [PubMed: 16351109]
19. Luo J, Xie Z, Lam JWY, Cheng L, Chen H, Qiu C, Kwok HS, Zhan X, Liu Y, Zhu D, Tang BZ. Chem Commun. 2001:1740–1741.
20. An BK, Kwon SK, Jung SD, Park SY. J Am Chem Soc. 2002; 124:14410–14415. [PubMed: 12452716]
21. Lim S-J, An B-K, Jung S-D, Chung M-A, Park SY. Angew Chem Int Ed. 2004; 43:6346–6350.
22. Ren Y, Lam JWY, Dong Y, Tang BZ, Wang KS. J Phys Chem B. 2005; 109:1135–1140. [PubMed: 16851072]
23. Kim S, Zheng Q, He GS, Bharali DJ, Pudavar HE, Baev A, Prasad PN. Adv Funct Mater. 2006; 16:2317–2323.
24. Qin A, Jim CKW, Tang Y, Lam JWY, Liu J, Mahtab F, Gao P, Tang BZ. J Phys Chem B. 2008; 112:9281–9288. [PubMed: 18630853]
25. He J, Xu B, Cheng F, Xia H, Li K, Ye L, Tian W. J Phys Chem C. 2009; 113:9892–9899.
26. Tong H, Hong Y, Dong Y, Häußler M, Lam JWY, Li Z, Guo Z, Guo Z, Tang BZ. Chem Commun. 2006:3705–3707.

27. Hong Y, Häußler M, Lam JWY, Li Z, Sin KK, Dong Y, Tong H, Liu J, Qin A, Renneberg R, Tang BZ. Chem Eur J. 2008; 14:6428–6437. [PubMed: 18512826]
28. Wang M, Zhang D, Zhang G, Zhu D. Chem Commun. 2008:4469–4471.
29. Zhao M, Wang M, Liu H, Liu D, Zhang G, Zhang D, Zhu D. Langmuir. 2009; 25:676–678. [PubMed: 19093755]
30. Li Z, Dong Y, Lam JWY, Sun J, Qin A, Häußler M, Dong Y, Sung HHY, Williams ID, Kwok HS, Tang BZ. Adv Funct Mater. 2009; 19:905–917.
31. Lu H, Xu B, Dong Y, Chen F, Li Y, Li Z, He J, Li H, Tian W. Langmuir. 2010; 26:6838–6844. [PubMed: 20112939]
32. Liu Y, Tang Y, Barashkov NN, Irgibaeva IS, Lam JWY, Hu R, Birimzhanova D, Yu Y, Tang BZ. J Am Chem Soc. 2010; 132:13951–13953. [PubMed: 20853831]
33. Liu Y, Deng C, Tang L, Qin A, Hu R, Sun JZ, Tang BZ. J Am Chem Soc. 2011; 133:660–663. [PubMed: 21171593]
34. Kim S, Pudavar HE, Bonoiu A, Prasad PN. Adv Mater. 2007; 19:3791–3795.
35. Kim S, Huang H, Pudavar HE, Cui Y, Prasad PN. Chem Mater. 2007; 19:5650–5656.
36. Liu J, Lam JWY, Tang BZ. J Inorg Organomet Polym. 2009; 19:249–285.
37. Kim S, Ohulchanskyy TY, Pudavar HE, Pandey RK, Prasad PN. J Am Chem Soc. 2007; 129:2669–2675. [PubMed: 17288423]
38. Wu W-C, Chen C-Y, Tian Y, Jang S-H, Hong Y, Liu Y, Hu R, Tang BZ, Chen C-T, Chen W-C, Jen AK-Y. Adv Funct Mater. 2010; 20:1413–1423.
39. Lim C-K, Kim S, Kwon IC, Ahn C-H, Park SY. Chem Mater. 2009; 21:5819–5825.
40. Tong H, Hong Y, Dong Y, Häußler M, Li Z, Lam JWY, Dong Y, Sung HH-Y, Williams ID, Tang BZ. J Phys Chem B. 2007; 111:11817–11823. [PubMed: 17877385]
41. Wang M, Zhang D, Zhang G, Tang Y, Wang S, Zhu D. Anal Chem. 2008; 80:6443–6448. [PubMed: 18576669]
42. Valeur, B. Molecular Fluorescence: Principle and Applications, Chapter 7. Wiley-VCH; Weinheim, Germany: 2002.
43. Kazuo S, Ryo H, Minoru S. J Polym Sci Part A: Polym Chem. 2000; 38:3369–3377.
44. Lu Z-R, Ye F, Vaidya A. J Control Release. 2007; 122:269–277. [PubMed: 17662500]
45. Cuchelkar V, Kopečková P, Kopeček J. Macromol Biosci. 2008; 8:375–383. [PubMed: 18215003]
46. Song HT, Choi JS, Huh YM, Kim S, Jun YW, Suh JS, Cheon J. J Am Chem Soc. 2005; 127:9992–9993. [PubMed: 16011350]
47. Lee J, Kim J, Park E, Jo S, Song R. Phys Chem Chem Phys. 2008; 10:1739–1742. [PubMed: 18350178]
48. Tian Y, Wu W-C, Chen C-Y, Strovas T, Li Y, Jin Y, Su F, Meldrum DR, Jen AK-Y. J Mater Chem. 2010; 20:1728–1736. [PubMed: 20454543]
49. Solntsev KM, McGrier PL, Fahrni CJ, Tolbert LM, Bunz UHF. Org Lett. 2008; 10:2429–2432. [PubMed: 18476714]
50. Nakatsuji S, Matsuda K, Uesugi Y, Nakashima K, Akiyama S, Katzer G, Fabian W. J Chem Soc, Perkin Trans. 1991; 2:861–867.
51. Demas JN, Grosby GA. J Phys Chem. 1971; 75:991–1178.
52. Joshi HS, Jamshidi R, Tor Y. Angew Chem Int Ed. 1999; 38:2721–2725.
53. Tominaga Y, Mizuse M, Hashidzume A, Morishima Y, Sato T. J Phys Chem B. 2010; 114:11403–11408. [PubMed: 20704303]
54. Morishima Y, Nomura S, Ikeda T, Seki M, Kamachi M. Macromolecules. 1995; 28:2874–2881.
55. Yin C, Li X, Wu Q, Wang J-L, Lin X-F. J Colloid Interface Sci. 2010; 349:153–158. [PubMed: 20621810]
56. Barz M, Luxenhofer R, Zentel R, Kabanov AV. Biomaterials. 2009; 30:5682–5690. [PubMed: 19631373]
57. Steinman RM, Mellman IS, Muller WA, Cohn ZA. J Cell Biol. 1983; 96:1–27. [PubMed: 6298247]

58. Lai MM, Hong JJ, Ruggiero AM, Burnett PE, Slepnev VI, De Camilli P, Snyder SH. J Biol Chem. 1999; 274:25963–25966. [PubMed: 10473536]
59. Gonda K, Komatsu M, Numata O. Cell Struct Funct. 2000; 25:243–251. [PubMed: 11129794]
60. Yuan A, Siu CH, Chia CP. Cell Calcium. 2001; 29:229–238. [PubMed: 11243931]
61. Beutner D, Voets T, Neher E, Moser T. Neuron. 2001; 29:681–690. [PubMed: 11301027]
62. Sankaranarayanan S, Ryan TA. Nat Neurosci. 2001; 4:129–136. [PubMed: 11175872]
63. Luo L, Tam J, Maysinger D, Eisenberg A. Bioconjugate Chem. 2002; 13:1259–1265.
64. Mosmann TJ. Immunol Methods. 1983; 65:55–63.
65. Carmichael J, Degraff WG, Gazdar AF, Minna JD, Michell JB. Cancer Res. 1987; 47:936–942. [PubMed: 3802100]

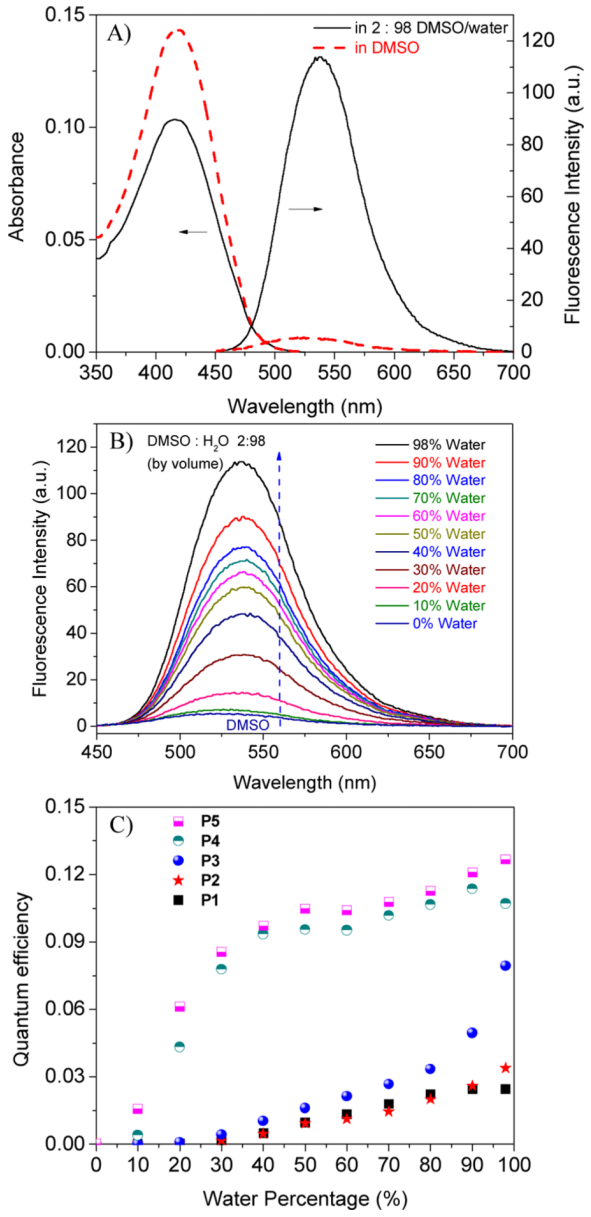


**Figure 1.**

A) Absorbance and emission spectra of a typical polymer **P3** in DMSO and 2% DMSO aqueous solution. B) Emission intensity change of **P3** in the mixture of DMSO and water. The spectra were excited at 405 nm. C) Quantum yields of polymers **P1** to **P5** in DMSO and water mixtures.

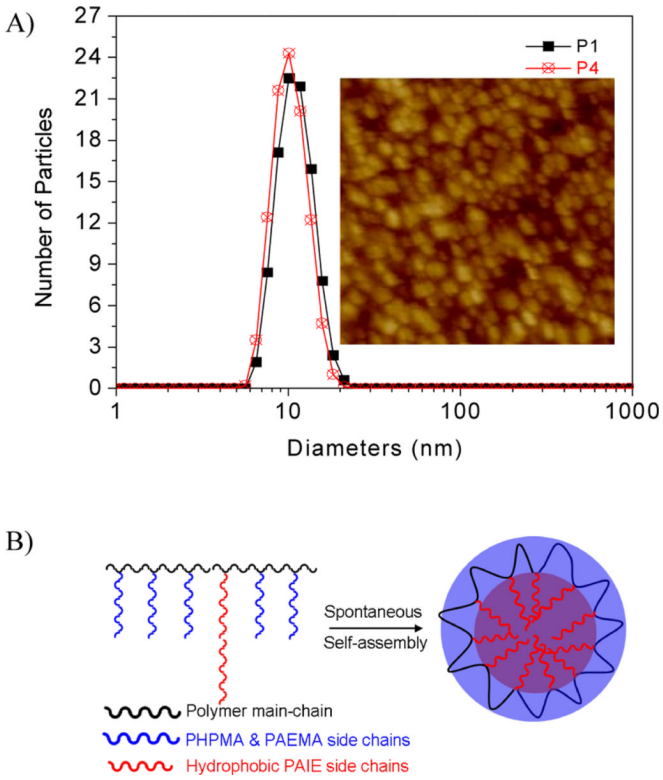


**Figure 2.**

A) Typical DLS of **P1** and **P4** in 2% DMSO aqueous solutions and the AFM image of **P4** (inserted, 0.75 μm × 0.75 μm). B) A possible schematic drawing of the micelles formed from the polymers using a “flower-micelle model”.

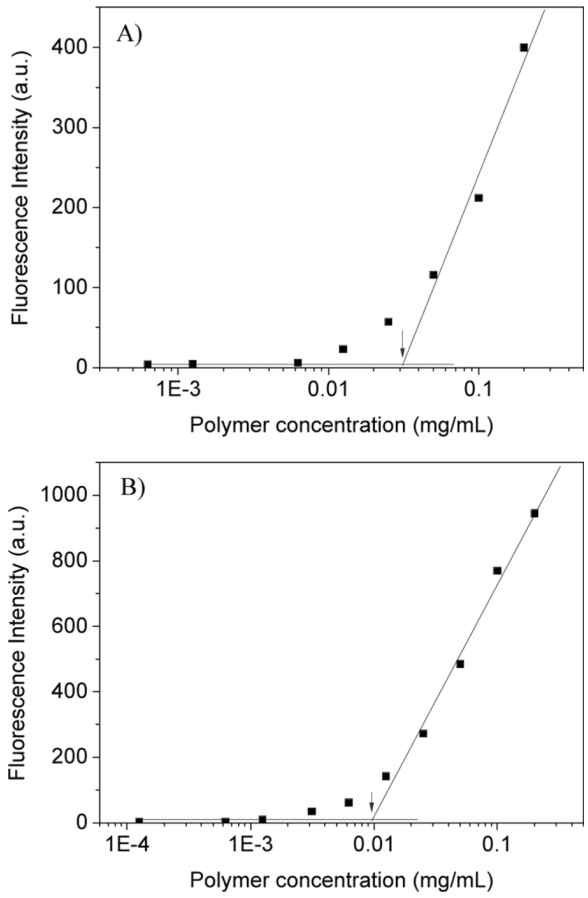


**Figure 3.**
Polymer concentration dependent fluorescence for CMC determination of **P1** (A) and **P4** (B) in aqueous solutions.

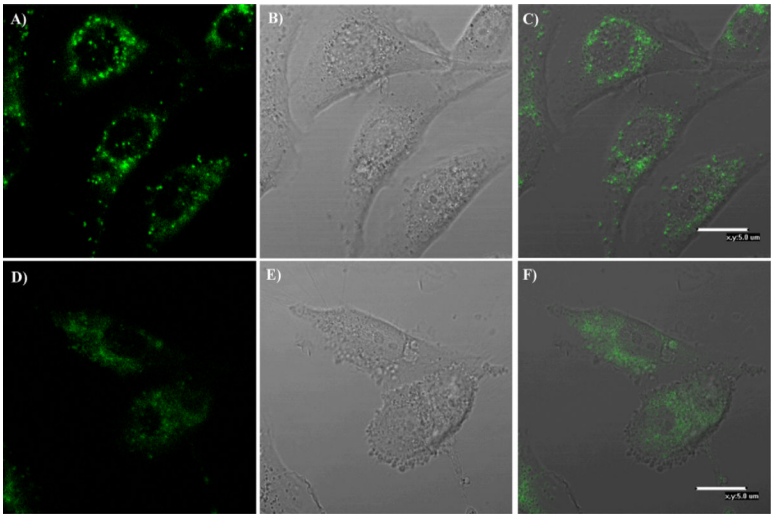


**Figure 4.**
Confocal fluorescence images of **P4** for CP-A (A, B, C) and U87MG (D, E, F). A and D are fluorescence images from the polymer. B and E are bright field images. C is the overlay of A and B. F is the overlay of D and E.

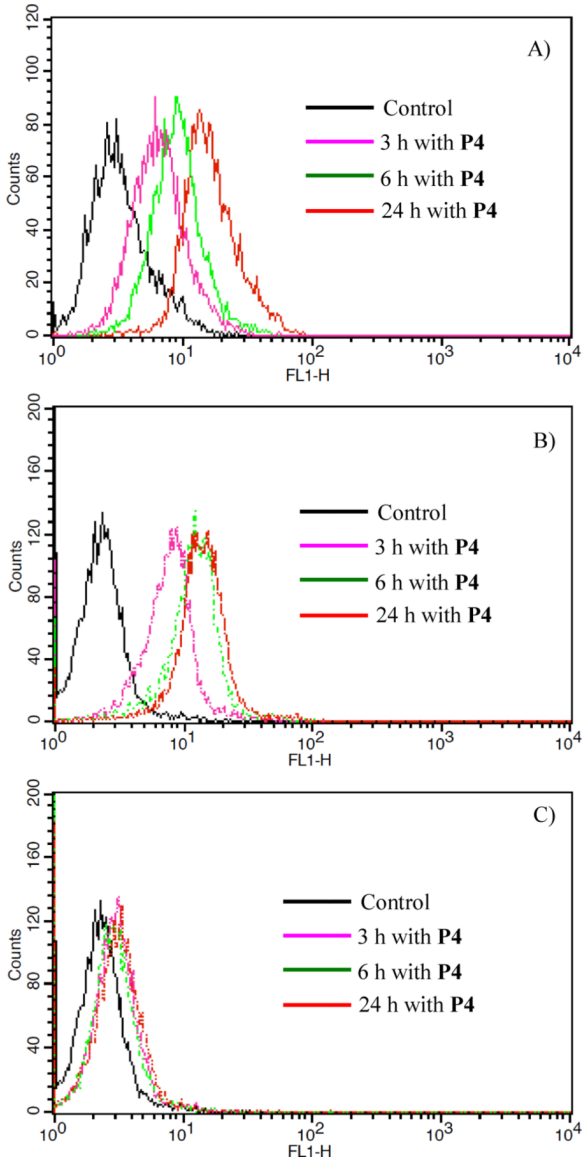


**Figure 5.**

A) Time dependent flow cytometry of **P4** by U87MG cells at 37 °C. B) Time dependent flow cytometry of **P4** by CP-A cells at 37 °C. C) Time dependent flow cytometry of **P4** by CP-A cells at 4 °C.

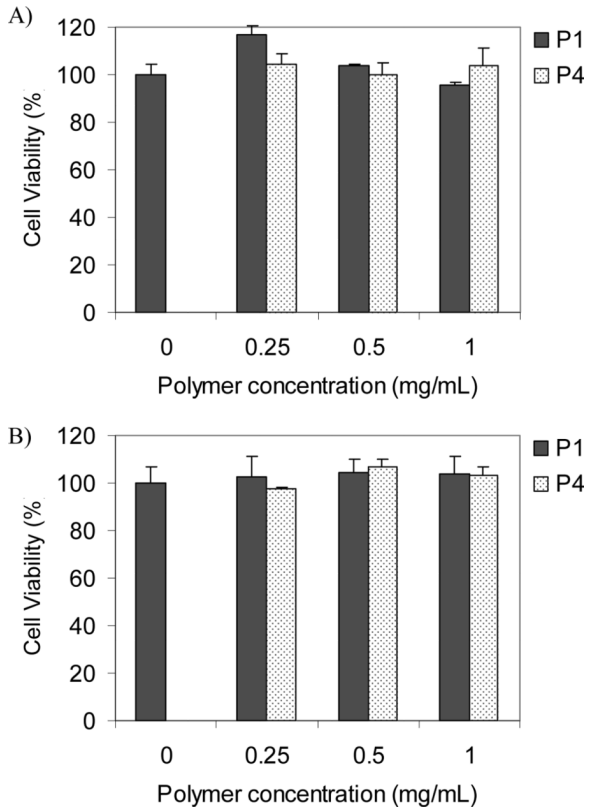


**Figure 6.**
Cytotoxicity of polymers **P1** and **P4** to U87MG (A) and CP-A (B) cells. Cellular internalization time is 24 hours at 37 °C.

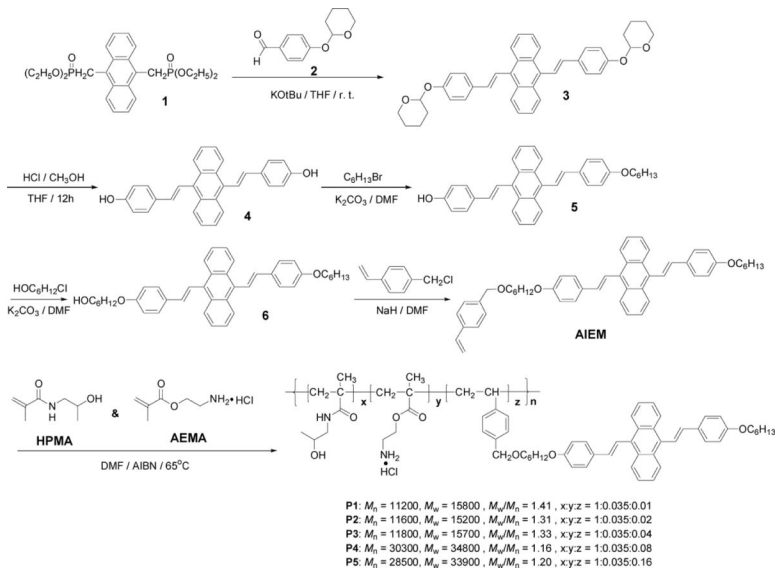


**Scheme 1.**
Synthesis of the AIE monomer (AIEM) and its copolymers.